

# Modulation of acyl-carnitines, the broad mechanism behind *Wolbachia*-mediated inhibition of medically important flaviviruses in *Aedes aegypti*

Gayathri Manokaran<sup>a,b,1</sup>, Heather A. Flores<sup>b</sup>, Conor T. Dickson<sup>a</sup>, Vinod K. Narayana<sup>c,d</sup>, Komal Kanojia<sup>c,d</sup>, Saravanan Dayalan<sup>c,d</sup>, Dedreia Tull<sup>c,d</sup>, Malcolm J. McConville<sup>c,d</sup>, Jason M. Mackenzie<sup>a</sup>, and Cameron P. Simmons<sup>a,b,e</sup>

<sup>a</sup>Department of Microbiology and Immunology, Peter Doherty Institute for Infection and Immunity, University of Melbourne, Parkville, VIC 3000, Australia; <sup>b</sup>Institute for Vector Borne Disease, Monash University, Clayton, Melbourne, VIC 3168, Australia; <sup>c</sup>Metabolomics Australia, Bio21 Molecular Science and Biotechnology Institute, University of Melbourne, Melbourne, VIC 3000, Australia; <sup>d</sup>Department of Biochemistry and Molecular Biology, University of Melbourne, Melbourne, VIC 3000, Australia; and <sup>e</sup>Oxford University Clinical Research Unit, Wellcome Trust Major Overseas Programme, District 5, Ho Chi Minh City, Vietnam

Edited by Richard J. Kuhn, Purdue Institute of Inflammation, Immunology, and Infectious Disease, West Lafayette, IN, and accepted by Editorial Board Member Diane E. Griffin July 17, 2020 (received for review September 6, 2019)

***Wolbachia*-infected mosquitoes are refractory to flavivirus infections, but the role of lipids in *Wolbachia*-mediated virus blocking remains to be elucidated. Here, we use liquid chromatography mass spectrometry to provide a comprehensive picture of the lipidome of *Aedes aegypti* (Aag2) cells infected with *Wolbachia* only, either dengue or Zika virus only, and *Wolbachia*-infected Aag2 cells superinfected with either dengue or Zika virus. This approach identifies a class of lipids, acyl-carnitines, as being down-regulated during *Wolbachia* infection. Furthermore, treatment with an acyl-carnitine inhibitor assigns a crucial role for acyl-carnitines in the replication of dengue and Zika viruses. In contrast, depletion of acyl-carnitines increases *Wolbachia* density while addition of commercially available acyl-carnitines impairs *Wolbachia* production. Finally, we show an increase in flavivirus infection of *Wolbachia*-infected cells with the addition of acyl-carnitines. This study uncovers a previously unknown role for acyl-carnitines in this tripartite interaction that suggests an important and broad mechanism that underpins *Wolbachia*-mediated pathogen blocking.**

*Wolbachia* | lipids | flavivirus

The discovery that introduction of *Wolbachia*, an endosymbiotic bacterium, into *Aedes aegypti* (*A. aegypti*) interferes with RNA virus replication has led to the deployment of *Wolbachia* as a tool for mosquito biocontrol (1, 2). Studies have shown that *Wolbachia* blocks the replication of arboviruses such as dengue virus (DENV), Zika virus (ZIKV), and chikungunya virus (1, 3, 4). With field trials demonstrating that *Wolbachia* are also capable of spreading through wild *A. aegypti* populations, *Wolbachia* biocontrol holds much promise in eliminating arbovirus transmission (1, 2). Multiple *Wolbachia* strains exist but only certain variants (*wMel*, *wAlbB*) block virus transmission without greatly impacting mosquito fitness (5–8). Currently, the release of *wMel A. aegypti* mosquitoes is being evaluated for its potential to control DENV transmission in several countries (including Brazil, Indonesia, Vietnam, Columbia, Australia) (9–12).

One mystery that remains unsolved is the mechanism behind *Wolbachia*-mediated virus blocking. Possible contributory factors include immune activation through the up-regulation of the reactive oxygen species (ROS)-dependent activation of Toll pathway genes and host microRNAs in *A. aegypti* (13–17). A comparative analysis of *Wolbachia* strains suggested the presence of a single mechanism of virus protection with a broad spectrum of virus inhibition (14). It has also been inferred that the degree of blocking conferred by different *Wolbachia* strains correlates with the density of those strains in key tissues, leading to the hypothesis that competition for host intracellular molecules underpins the virus blocking mechanism (6, 14, 18). Indeed, supplementation with cholesterol in *Drosophila* and mosquito cell lines containing *Wolbachia* increased

virus replication, implying that both virus and *Wolbachia* may be competing for cholesterol (19, 20). Other groups have shown that *Wolbachia*-infected mosquito cells had perturbed cellular lipid profiles and up-regulation of the fatty acid synthase (FAS) and Acyl-CoA thioesterase (ACOT) enzymes, resulting in increased complex lipid synthesis and fatty acyl-CoAs (FA-CoA) catabolism (16, 20–22). Together these studies suggest that the lipidome is significantly altered with *Wolbachia* infection and may consequently affect the capacity for viral infection.

*Flaviviridae* such as DENV, West Nile virus (WNV), and hepatitis C virus rely heavily on cellular lipids during replication (23–25). Not only are the lipids integrated into virus-induced structures, but virus replication has been shown to alter cellular metabolism profoundly, including increases in fatty acid and cholesterol biosynthesis and up-regulation of the host FAS enzyme (26–29). Lipidomic studies on DENV-infected mosquitoes, mosquito cells, and whole WNV virions have identified discrete

## Significance

***Wolbachia* (*wMel* strain)-infected *Aedes aegypti* mosquitoes are refractory to disseminated arboviral infections. Yet previous studies into the mechanism behind *Wolbachia*-mediated virus blocking have not considered the involvement of lipids, apart from cholesterol, during superinfection. We used liquid chromatography mass spectrometry to study the lipidome in mosquito cells infected with virus, *wMel*, or superinfected with both virus and *wMel*. Interestingly, a class of lipids, acyl-carnitines increased during virus infection but remained low with *wMel*. These findings uncover a previously unknown role for acyl-carnitines in the interaction among virus, *wMel*, and cells, suggesting a mechanism underlying *Wolbachia*-mediated pathogen blocking. Importantly, this study supports *Wolbachia* introgression into *A. aegypti* populations as a biocontrol method to reduce arboviral (e.g., DENV) transmission.**

Author contributions: G.M., D.T., J.M.M., and C.P.S. designed research; G.M., H.A.F., C.T.D., V.K.N., and K.K. performed research; V.K.N., K.K., S.D., D.T., and M.J.M. contributed new reagents/analytic tools; G.M., H.A.F., V.K.N., S.D., J.M.M., and C.P.S. analyzed data; G.M. wrote the paper; D.T. provided advice and troubleshooting on LCMS data; and M.J.M. advised on LCMS experiments.

The authors declare no competing interest.

This article is a PNAS Direct Submission. R.J.K. is a guest editor invited by the Editorial Board.

This open access article is distributed under [Creative Commons Attribution-NonCommercial-NoDerivatives License 4.0 \(CC BY-NC-ND\)](https://creativecommons.org/licenses/by-nc-nd/4.0/).

<sup>1</sup>To whom correspondence may be addressed. Email: [gayathri.manokaran@monash.edu](mailto:gayathri.manokaran@monash.edu).

This article contains supporting information online at <https://www.pnas.org/lookup/suppl/doi:10.1073/pnas.1914814117/-DCSupplemental>.

First published September 10, 2020.

alterations of the lipidome during infection (25, 30, 31). Any *Wolbachia*-mediated alterations to the cellular lipidome that are not favorable would undeniably affect virus replication.

To gain insights into the *Wolbachia*-mediated virus blocking mechanism, we used liquid chromatography mass spectrometry (LCMS) to examine changes in the cellular lipidome upon combinations of

infection with *wMel*, DENV, and ZIKV. Our results demonstrated significant fluctuations in various lipids that function as membrane building blocks, energy intermediates, and lipids involved in biosynthesis and lipolysis pathways. One prominent observation involves a class of lipids known as acyl-carnitines. Our results demonstrate that *wMel* modulates acyl-carnitine levels

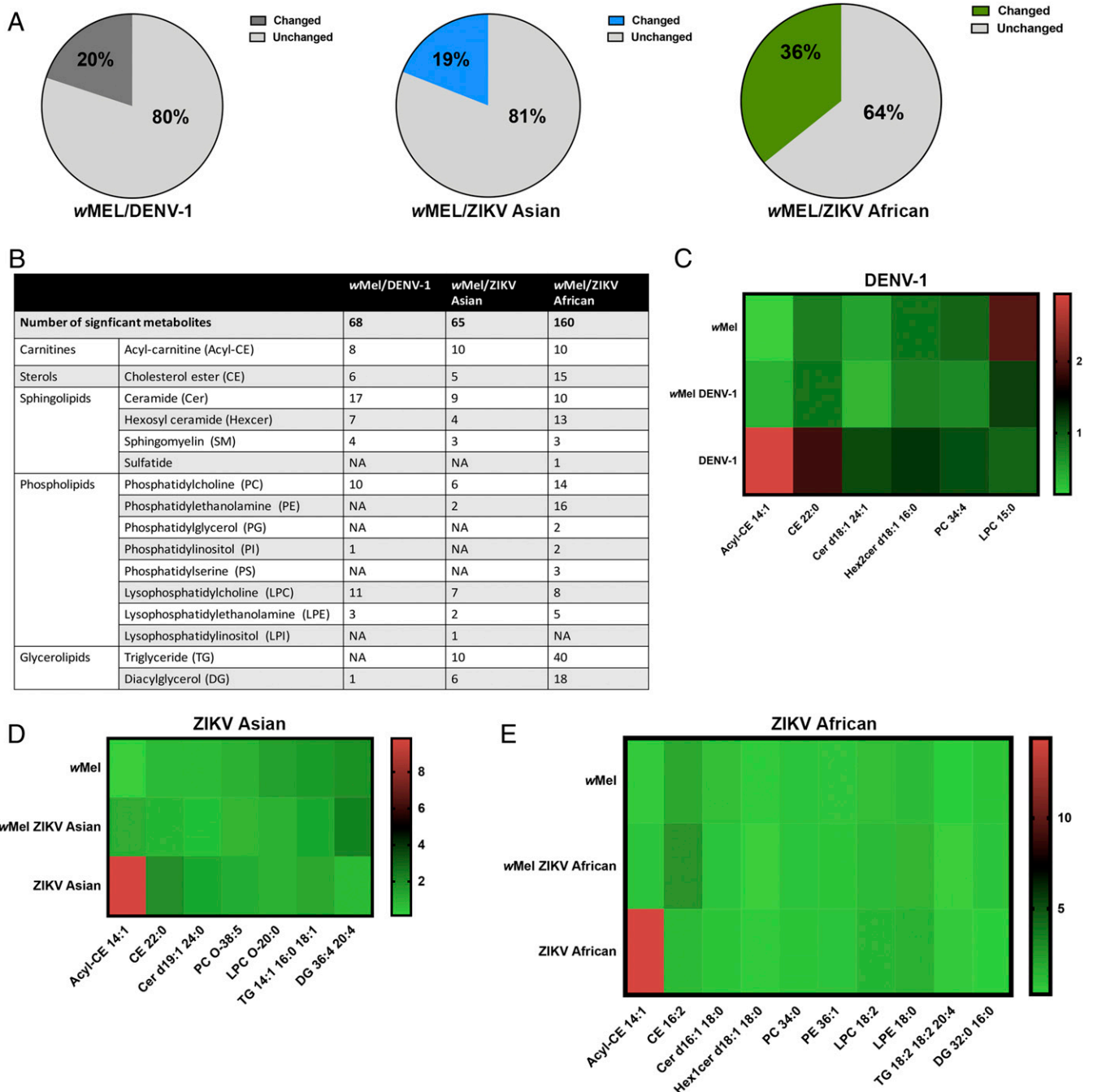


**Fig. 1.** Results from LCMS analysis of the mosquito cellular lipidome upon infection *wMel*/arbovirus infection. (A) Pie charts showing the percentages of the cellular lipidome changed upon superinfection of *Aag2.wMel* cells with Dengue-1 (DENV-1), Zika African (ZIKV African) and Zika Asian (ZIKV Asian) viruses in comparison to uninfected cells. (B) Table listing the number of metabolites significantly modulated under the three experimental conditions (*wMel*/DENV-1, *wMel*/ZIKV Asian, *wMel*/ZIKV African) and the various lipid classes they belong to. (C–E) Heatmaps illustrating normalized metabolites, each representative of its lipid class under three conditions: *wMel* infection only, virus infection only, and *wMel*/virus infection. Briefly, metabolites that were significantly modulated during superinfection with virus/*wMel* were grouped into lipid classes (Dataset S2). Lipid classes with <5 significant metabolites were excluded. An example was then selected to depict the pattern of abundance of each lipid class under each infection condition. After selection, fold changes were calculated based on measures of the specific metabolite during infection expressed as a ratio against that metabolite in uninfected cells. This data were applied to heatmaps for easy interpretation of the common changes seen in the lipidome. DENV-1 (C), ZIKV Asian (D), ZIKV African (E).

in mosquito cells, which is highly detrimental to both ZIKV and DENV replication. In conclusion, our findings provide evidence that a *Wolbachia*-modulated lipidome contributes toward flavivirus resistance. Additionally, we uncover a previously unknown role of acyl-carnitines in this tripartite interaction that suggests an important and broad mechanism that underpins *Wolbachia*-mediated pathogen blocking.

## Results

**The Mosquito Cell Lipidome Is Significantly Altered by *w*Mel and Virus Infection.** To investigate if the mosquito lipidome is involved in the *Wolbachia*-mediated virus blocking mechanism, we undertook a whole-cell lipidomics approach. Briefly, *Aag2.w*Mel and *Aag2.TET* cells were infected with DENV-1 and two different strains of ZIKV (Zika Asian and Zika African) and extracted for LCMS analysis 48 h postinfection (48 h.p.i.) (SI Appendix, Figs. S1 and S2). LCMS targeted lipidomic analysis resulted in the identification of a total of 335 lipids across five major lipid classes: phospholipids, sphingolipids, glycerolipids, sterols, and carnitines (Dataset S1). The abundance of these lipids under the various conditions (*w*Mel infection only, *w*Mel/virus infection, virus infection only, and the no-infection control) is shown in Dataset S1 (SI Appendix). These features were subjected to statistical analysis to simultaneously compare the differences in metabolite abundance among three datasets: *w*Mel-infected and uninfected cells, virus-infected and uninfected cells, and *w*Mel/virus-infected cells and uninfected cells. Lipids showing statistically significant differences in abundance ( $P < 0.05$ ) were identified (SI Appendix, Fig. S3 and Dataset S2).

Relative to uninfected cells, 20%, 19%, and 36% of the total lipids were altered in abundance in *w*Mel/DENV-1, *w*Mel/ZIKV Asian, and *w*Mel/ZIKV African conditions, respectively (Fig. 1A). There were significant changes in various lipid classes, but a majority of the changes were in phospholipids and sphingolipids (Fig. 1B). Data from the heatmap analysis showed that acyl-carnitines, cholesterol esters, and sphingolipids were generally up-regulated during virus infection but decreased in abundance with *w*Mel infection (Fig. 1C–E). The exception was ZIKV African, which resulted in an increase in acyl-carnitines but not cholesterol esters or sphingolipids (Fig. 1E). There were no distinct patterns of change in phospholipid abundance (Fig. 1C–E). Both Zika viruses caused a decrease in DGs, but coinfection with *w*Mel increased the DG levels (Fig. 1D and E). In contrast, DENV-1 infection did not modulate the glycerolipids significantly (Fig. 1B). In summary, acyl-carnitines, cholesterol esters, sphingolipids, and DGs are modulated differently during virus infection as compared to *w*Mel infection, thus suggesting that these lipid classes may be implicated in the mechanism of virus blocking.

**Acyl-Carnitines Increase Significantly upon Infection with Three Viruses but Remain Down-Regulated during *w*Mel Infection.** We tested for significant lipids that were common to infection by all three viruses in *Aag2.w*Mel cells. Remarkably, we discovered that only 12 lipid moieties were significantly altered in *Aag2.w*Mel cells during infection with DENV-1, ZIKV African, and ZIKV Asian as compared to uninfected cells (Fig. 2A and B). Significantly modulated lipids comprised of a lysophospholipid LPE 18:0, three sphingolipids, (Hex1cer d-16:1 18:0, Hex1cer d-18:2 24:0, and Hex2cer d18:1 24:0) and eight acyl-carnitines. Acyl-carnitines are intermediate molecules that shuttle fatty acyl-CoA from the cytoplasm into the mitochondria for  $\beta$ -oxidation and subsequent energy (ATP) production.

To further investigate the changes in acyl-carnitines, we compared *w*Mel-infected, virus-infected, and *w*Mel/virus-infected cells to uninfected cells. We observed that the levels of most acyl-carnitines were consistently lower (below basal fold change of 1) upon *w*Mel infection as compared to uninfected cells (Fig. 2C). On the contrary, infection with all three viruses results in elevated levels of most acyl-carnitines, with fold changes ranging from 1.1

to 14 (Fig. 2D). However, upon superinfection with *w*Mel and virus, we observed a drastic reduction in a majority of the acyl-carnitines, with the average fold change below the basal level of 1 (Fig. 2E). This provided further evidence that *Wolbachia* might be modulating levels of acyl-carnitines, which might impact virus replication.

**Inhibiting Acyl-Carnitines Results in Abolished Virus Replication in Human Cells.** To test if elevated acyl-carnitine levels are required during virus infection, we next examined the impact of a widely used acyl-carnitine inhibitor, etomoxir, on infection with DENV-1 and ZIKV Asian (the more epidemiologically relevant ZIKV strain). Etomoxir is a small molecule inhibitor that irreversibly inhibits carnitine palmitoyl-transferase 1a (CPT1a), the mitochondrial enzyme responsible for the formation of acyl-carnitines (32, 33). Through LCMS analysis, we first confirmed that etomoxir treatment reduces levels of most acyl-carnitines but also causes global changes in the cellular lipidome (SI Appendix, Figs. S4 and S5). As compared to untreated cells, dramatically reduced viral RNA and plaque titers were observed in etomoxir-treated human cells for both ZIKV Asian and DENV-1 (Fig. 3). In fact, replication was almost abolished in treated cells, suggesting that acyl-carnitines are crucial in the virus lifecycle (SI Appendix, Figs. S3 and S4).

**Etomoxir Treatment of *A. aegypti* Elevates *w*Mel Levels but Restricts Virus Replication.** Our findings suggested that acyl-carnitines are important for virus replication. To test if *w*Mel might be limiting virus replication in mosquitoes by affecting acyl-carnitine levels, *A. aegypti* mosquitoes reared with etomoxir were tested for *w*Mel density and DENV blocking. Surprisingly, *w*Mel densities in both heads/thoraxes and abdomens were significantly elevated upon etomoxir treatment (Fig. 4A and B). The difference in levels was more evident in the abdomen than in the heads/thoraxes (Fig. 4A and B) (34). These results collectively suggest that *w*Mel thrives in an environment with reduced acyl-carnitines. There was no difference in DENV-2 RNA levels between etomoxir-treated and untreated *w*Mel *A. aegypti*: both groups restricted DENV replication similarly (Fig. 4C). However, there was a significant 3.5-fold reduction of DENV copies in etomoxir-treated Tet-control mosquitoes as compared to untreated Tet-control mosquitoes (Fig. 4C). This reduction, although significant, was not as high as the DENV restriction observed in *w*Mel mosquitoes (Fig. 4C). Taken together, this confirmed that the effect on acyl-carnitines by *w*Mel could be one contributory factor that blocks virus replication in *w*Mel-infected mosquitoes.

**Provision of Acyl-Carnitines to *Aag2.w*Mel Cells Increased Virus Replication.** To further test if *Wolbachia*-mediated virus blocking is dependent on acyl-carnitines, we used commercially available acyl-carnitines to study *w*Mel density and virus replication in *Aag2.w*Mel and *Aag2.TET* cells. The relative *w*Mel density significantly dropped from 10 to 2.5, with the addition of exogenous acyl-carnitines to *Aag2.w*Mel cells (Fig. 5A). This further confirmed that *w*Mel prefers an environment with reduced acyl-carnitines. We next measured virus replication in *Aag2.w*Mel cells with the provision of exogenous acyl-carnitines. Our results revealed that DENV-1, ZIKV Asian, and ZIKV African plaque titers increased at least twofold and viral RNA levels in *Aag2.w*Mel cells increased about onefold to twofold with the addition of exogenous acyl-carnitines (Fig. 5B and C). As expected, the plaque titers and viral RNA levels increased in treated cells as compared to untreated cells even in the absence of *w*Mel, further confirming that acyl-carnitines are crucial in virus infection (Fig. 5B and C). Taken collectively, these data indicate that virus replication in *w*Mel-infected cells can be increased by addition of acyl-carnitines, further supporting the hypothesis that acyl-carnitines are directly involved in the *Wolbachia*-mediated virus blocking mechanism.

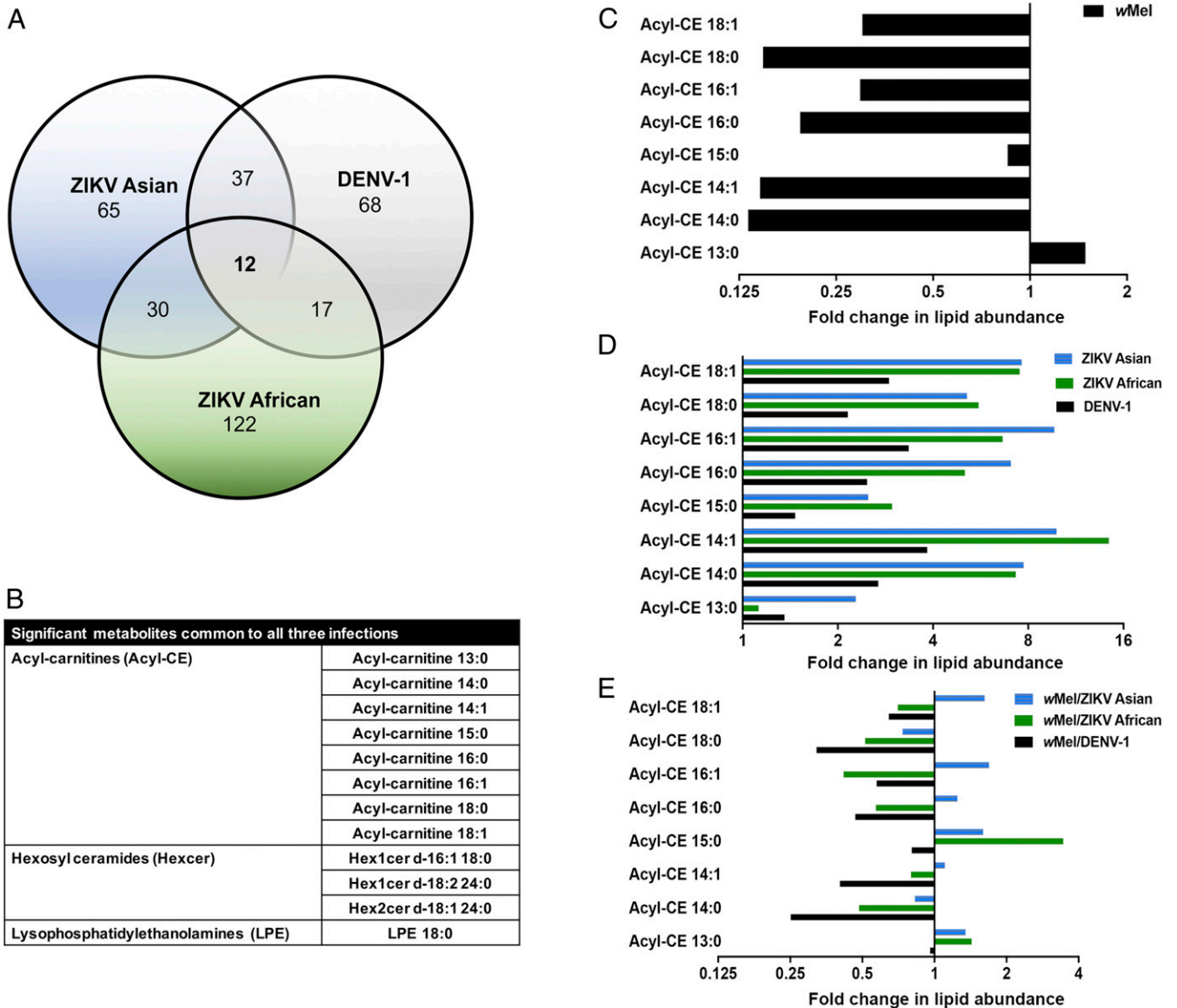


**Fig. 2.** Role of acyl-carnitines in virus superinfection of *Aag2.wMel* cells. (A) Venn diagram displaying the number of metabolites significantly altered ( $P < 0.05$ ; in comparison to uninfected cells) in *Aag2.wMel* cells superinfected with DENV-1 or ZIKV Asian or ZIKV African. (B) Table showing metabolites common to superinfection with all three viruses in *wMel*-infected cells. (C–E) Bar charts showing the fold changes in acyl-carnitines during infection with *wMel* only (C), virus only (D), and *wMel*/virus (E). Fold changes shown are measures of the specific metabolite during infection expressed as a ratio against that metabolite in uninfected cells.

**Proposed Model Depicting the Mechanism behind *Wolbachia*-Mediated Blocking.** Based on our findings, we propose a model for the mechanism behind *Wolbachia*-mediated blocking (Fig. 6). During flavivirus infection, FA-CoAs (activated fatty acids) are converted to acyl-carnitines for transport into the mitochondria for  $\beta$ -oxidation and subsequent energy production (Fig. 6). Mitochondrial  $\beta$ -oxidation results in the production of ATP and acetyl (C2)-CoA (Fig. 6). The resulting ATP might be used as the energy source to produce more virions, and acetyl (C2)-CoA can be used for de novo synthesis of longer chain FA-CoA molecules at the site of virus replication (27, 30, 35). Indeed, several studies have shown that increased  $\beta$ -oxidation is vital for flavivirus replication (35–37). Such elevated energetic demands during virus infection might lead to large amounts of FA-CoAs entering the mitochondria but only partially being broken down by  $\beta$ -oxidation, which becomes a bottleneck for this reaction. This mitochondrial overload results in an accumulation of acyl-carnitines (Fig. 6). Thus, the increased

levels of acyl-carnitines observed are important and necessary for efficient flavivirus replication.

However, when *Wolbachia* is present, it modulates acyl-carnitine levels by driving the metabolic force in the opposite direction (Fig. 6). This is likely due to *Wolbachia* redirecting the energy source for either the production of bacteria-specific lipids or *Wolbachia*-driven energy production. The immense reduction in acyl-carnitines caused by *wMel* renders flavivirus replication highly inefficient in *wMel*-infected mosquito cells as downstream  $\beta$ -oxidation is dramatically reduced (Fig. 6). Reducing and sustaining the low acyl-carnitine levels could thus be detrimental to many viruses, as it interferes with FA-CoA metabolism, the primary hub integrating multiple lipid metabolic pathways. We suggest that these opposing metabolic driving forces result in competition between the endosymbiont *wMel* and virus and encompass a broad mechanism of *Wolbachia*-mediated virus blocking.

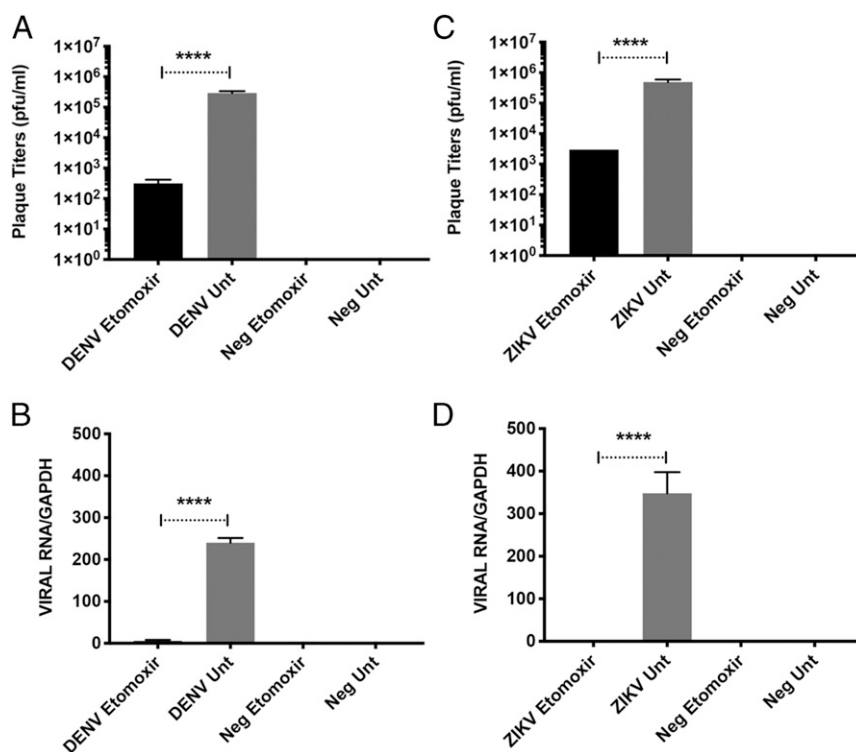


**Fig. 3.** Effects of etomoxir, an irreversible acyl-carnitine inhibitor, on replication of dengue and Zika virus. HuH-7 cells were treated with 200  $\mu$ M etomoxir, a widely used irreversible inhibitor of acyl-carnitines, for 48 h after which virus was added at MOI 5. Virus supernatant and cellular RNA were harvested at 24 h.p.i. for plaque assays and qRT-PCR. All results from qRT-PCR were normalized against GAPDH. (A) Plaque titers following DENV infection. (B) Expression levels of DENV RNA using primers targeting 3' UTR. (C) Plaque titers following ZIKV Asian infection. (D) Expression levels of ZIKV Asian RNA using primers targeting NS5. Data are represented as mean  $\pm$  SEM; \*\*\*\* $P$  < 0.0001, two-tailed Student's  $t$  test.

## Discussion

*Wolbachia* has been introduced into mosquitoes to successfully prevent the spread of clinically important arboviruses, yet the mechanisms by which *Wolbachia* block virus transmission are not fully understood. Using a whole-cell lipidomics approach, here we report the involvement of acyl-carnitines, a class of lipids previously unknown to play a crucial role in *Wolbachia*-mediated virus blocking. Acyl-carnitines are important intermediate molecules that transport FA-CoA from the cytoplasm to the mitochondria for  $\beta$ -oxidation and, consequently, ATP production.

We observed a significant increase in acyl-carnitine levels upon ZIKV and DENV infection of *Aag2*.TET cells. Using an acyl-carnitine inhibitor, etomoxir, we also showed significant reduction in flavivirus replication in human cells. We found that etomoxir causes global changes in the lipidome, which could be attributed to off-target effects or overstimulation of compensatory lipid pathways caused by the irreversible effect on CPT1a (38, 39). As the lipidome and cellular metabolism consists of elaborate networks of closely interconnected pathways, it is impossible to disrupt acyl-carnitine levels without affecting downstream lipid profiles or energy production. We recognize that this is a drawback of working on the lipidome. However, considering that we have already studied other global changes in the lipidome before with the superinfection experiment (Figs. 1 and 2) and identified acyl-carnitines to be of interest, it is unlikely that other changes caused in the lipidome by the use of etomoxir would be relevant to the ultimate aim of this study. Since our goal was to directly block the formation of acyl-carnitines and as etomoxir treatment did significantly deplete most acyl-carnitines (SI Appendix, Fig. S5), we concluded that etomoxir treatment did provide valuable insights into the behavior of *wMel* and the viruses when acyl-carnitine levels are disrupted.

Consistent with our findings, a recent study demonstrated a remarkable accumulation of acyl-carnitines in mosquito midguts upon DENV infection (30). Elevated acyl-carnitine levels during virus infection could be attributed to mitochondrial overload. Due to elevated energetic demands during virus infection, an increased amount of FA-CoA continuously enter the mitochondria but are only partially broken down by  $\beta$ -oxidation, which becomes a bottleneck in this pathway. This results in a corresponding increase in acyl-carnitines, upstream of  $\beta$ -oxidation (30).

Our data revealed that depleting acyl-carnitines in mosquitoes resulted in significantly higher levels of *wMel*. Interestingly, it has been previously demonstrated that *Wolbachia* can increase FA-CoA (activated fatty acid) catabolism by increasing the expression of ACOT enzymes (22). Taken together, this suggests that *Wolbachia* drives the conversion of FA-CoA to free fatty acids, thereby resulting in decreased acyl-carnitine levels. As acyl-carnitines are involved in ATP/energy generation from lipids, this depletion might result in a general decline in  $\beta$ -oxidation and ATP production. Indeed, measurement of cellular ATP generation showed a significant reduction of ATP levels in the presence of *wMel* (SI Appendix, Fig. S6). Reduced ATP levels would affect virus replication too, as virus replication is energetically demanding. Although it remains unclear why *Wolbachia* redirects this pathway, it might be for the production of bacteria-specific lipids or *Wolbachia*-driven energy production. It is noteworthy that the *wMel*-induced reduction in acyl-carnitine levels does not lead to a massive fitness cost in mosquitoes. A recent study showed that *Wolbachia* subverts the endoplasmic reticulum to acquire their vacuolar membrane and colonize the host cell at high density without triggering endoplasmic reticulum stress or compromising host cell viability (40). This suggests that the presence of *Wolbachia*,

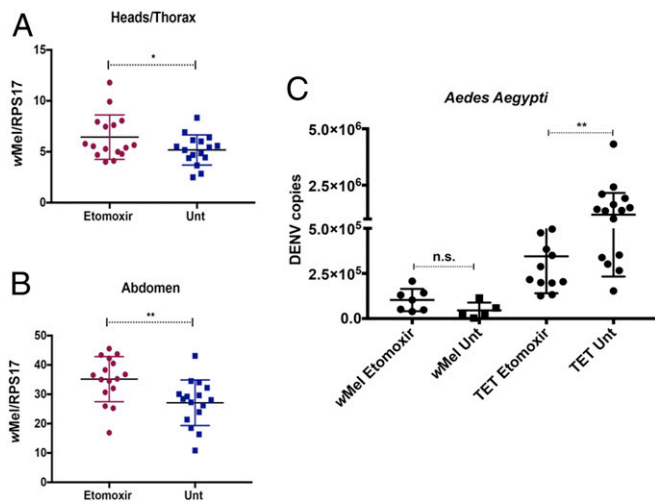


**Fig. 4.** Effects of acyl-carnitine depletion on wMel and superinfection with dengue in *A. aegypti* mosquitoes. wMel *A. aegypti* mosquito larvae were reared in water alone or in water containing 100  $\mu$ M etomoxir. Three days postemergence, female mosquitoes were collected for testing of *Wolbachia* density. Individual, female mosquitoes from each sample group were dissected to separate the abdomens from the heads/thoraxes. DNA was extracted and subjected to qPCR. Primers used targeted the *Wolbachia* surface protein, and results were normalized against the single-copy mosquito *rps17* gene. Blue squares represent untreated mosquitoes, and red dots represent treated mosquitoes. (A) *Wolbachia* densities in the heads/thoraxes of treated versus untreated mosquitoes. (B) *Wolbachia* densities in abdomens of treated versus untreated mosquitoes. (C) Treated and untreated wMel and Tet-control adult female mosquitoes (7 d old) were injected with  $3.4 \times 10^5$  TCID<sub>50</sub>/mL of DENV-2. Mosquitoes were incubated for 7 d before total RNA extraction was performed on entire mosquitoes, followed by DENV qRT-PCR. DENV absolute quantities were determined by extrapolation from an internal standard curve generated from plasmid DNA encoding the conserved 3' UTR sequence. TET: mosquitoes from a tetracycline-treated line to deplete wMel completely; Unt: untreated; wMel: mosquitoes with wMel infection. Data are represented as mean  $\pm$  SEM; \* $P < 0.05$ ; \*\* $P < 0.01$ ; n.s.: not significant, two-tailed Student's *t* test.

while causing changes, does not perturb the tightly regulated mechanisms of cell homeostasis.

Our model suggests that modulation of acyl-carnitines by *Wolbachia* is an important and broad mechanism behind virus blocking. Indeed, provision of exogenous acyl-carnitines increased the infection of all three viruses in wMel cell, although not to the same extent. Unfortunately, these increases were not substantial as there is no commercially available general acyl-carnitine compound that can be used in place of the eight identified acyl-carnitines in Fig. 2. The supplemented acyl-carnitines may not be important to virus replication but were used since they were the only commercially available compounds. It is also unclear which stage of virus replication acyl-carnitines are needed for. To elucidate the “extent” of this increased replication in wMel cells was difficult too, given that viruses depend on acyl-carnitines even in the absence of wMel.

To date, there has been one other lipidomic study of *Wolbachia*-infected cells published (21). This study was conducted on *Aedes albopictus* Aa23 cells and compared cellular lipidomic profiles between *Wolbachia*-infected and uninfected cells (21). Virus infection was not performed (21). Their data showed substantial shifts in the cellular lipid profile, a depletion of sphingolipids, some reductions in diacylglycerols, and phosphatidylcholines in *Wolbachia*-infected cells (21). Consistent with this study, we observed depletion of some sphingolipids, particularly ceramides during wMel infection (Dataset S1). However, there were no notable reductions in diacylglycerols or phosphatidylcholines (Dataset S1).

Additional mechanisms for the pathogen blocking phenotype of *Wolbachia* have been proposed. The down-regulation of insulin receptor kinase activity in *Wolbachia*-positive cells was recently shown to contribute to blocking of virus replication (41). Inhibition of the insulin receptor thus impaired insulin signaling, leading to reduced virus replication (41). Interestingly, acyl-carnitines have been associated with insulin resistance (42). During metabolic overload, when there is incomplete  $\beta$ -oxidation, the intramitochondrial accumulation of intermediates such as acyl-carnitines could result in impaired insulin signaling (42). The modulation of cholesterol and lipid homeostasis in the presence of *Wolbachia* may also contribute toward the pathogen-blocking effect as virus would have limited access to these metabolites essential for replication (19–21). Interestingly, several hits from our lipidomic study pertain to signaling pathways that may be highly relevant to at least some of these proposed mechanisms.

In brief, our study suggests that the down-regulation of acyl-carnitines in the presence of *Wolbachia* is one mechanism contributing to its pathogen blocking “syndrome” and provides initial insights into the importance of the metabolic environment

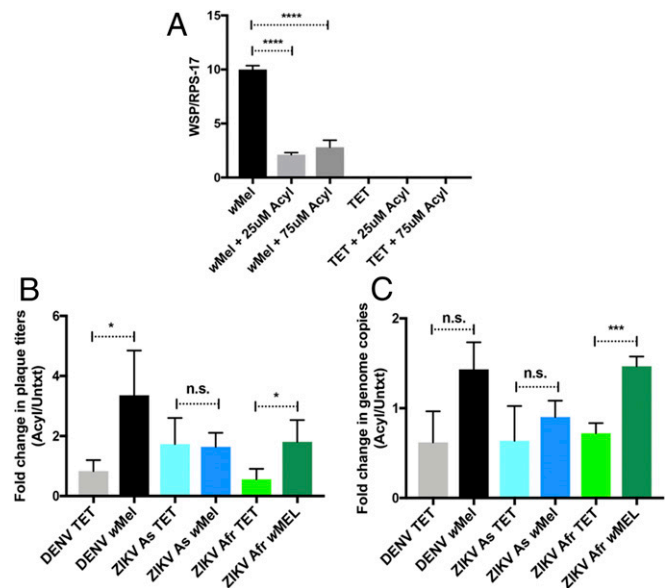


**Fig. 5.** Effects of addition of commercially available acyl-carnitines on flavivirus superinfection of wMel-infected cells. (A) *Aag2.wMel* and *Aag2.TET* cells were seeded onto plates and treated with a combination of commercially available acyl-carnitines or untreated. Concentrations shown (in micromolar) are the concentration of each acyl-carnitine added per well. Relative density of wMel is displayed, 3 d posttreatment. Primers used targeted the *Wolbachia* surface protein (WSP), and results were normalized against the single-copy mosquito *rps17* gene. (B and C) *Aag2.wMel* and *Aag2.TET* cells were infected with DENV (MOI 1), ZIKV Asian (MOI 0.1), and ZIKV African (MOI 0.2) viruses. At 24 h.p.i., three commercially available carnitines, each at a concentration of 25  $\mu$ M, were mixed and added to infected cells (49). Untreated cells (no added acyl-carnitines) were used as controls. Virus supernatant and cellular RNA were harvested at 96 h.p.i. Abbreviation “Acyl” represents the mixture of acyl-carnitines added. “Untxt” represents no treatment. TET: cells from a tetracycline-treated line to deplete wMel completely; wMel: cells with wMel infection. Results from at least three independent experiments are represented. Data are represented as mean  $\pm$  SEM; \* $P < 0.05$ ; \*\*\* $P < 0.001$ ; \*\*\*\* $P < 0.0001$ ; n.s.: not significant. (B) Fold change of plaque titers in the treated samples (Acyl) versus the untreated samples (Untxt) are shown. (C) Fold change of the relative expression of viral RNA levels in the treated samples (Acyl) versus the untreated samples (Untxt) are shown. All viral RNA levels were normalized against the mosquito housekeeping gene (*rps17*). Specific primers were used for each virus: Primers for DENV targeted the 3' UTR, and primers for ZIKV Asian and ZIKV African targeted N5S.

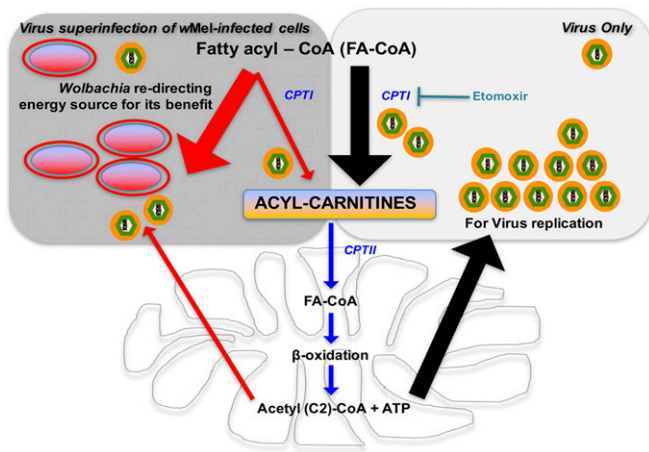


**Fig. 6.** Proposed model depicting the mechanism behind *Wolbachia*-mediated blocking. Flavivirus infection results in FA-CoAs (activated fatty acids) being converted to acyl-carnitines for transport into the mitochondria for  $\beta$ -oxidation. Mitochondrial  $\beta$ -oxidation results in production of ATP (energy that might be redirected to produce novel virions) and acetyl (C2)-CoA (that can be recycled to synthesize longer chain FA-CoA at site of viral replication). Such elevated energetic demands might lead to the accumulation of acyl-carnitines due to mitochondrial overload. Increased levels of acyl-carnitines are important and necessary for efficient virus replication. When *Wolbachia* is present, acyl-carnitine levels are modulated, driving the metabolic force in the opposite direction. This is likely due to *Wolbachia* redirecting the energy source for either the production of bacteria-specific lipids or *Wolbachia*-driven energy production. This immense reduction in acyl-carnitines caused by *wMel* renders virus replication highly inefficient in the presence of *Wolbachia* as downstream  $\beta$ -oxidation is dramatically reduced. Black arrows depict the scenario during virus infection, and red arrows depict the pathway altered in the presence of *Wolbachia*.

during this tripartite interaction. Along with recent reports, this finding provides further reassurance that *Wolbachia* biocontrol may be highly effective in controlling arbovirus transmission in future as arboviruses would not be able to easily evolve to escape this phenomenon of reduced cellular resources (2, 43).

## Materials and Methods

**Cells, Viruses, and Infections.** Huh-7, C6/36, and BHK-21 cells were obtained from the American Type Culture Collection and cultured accordingly. *Aag2.wMel* cells, infected with the *wMel* strain of *Wolbachia*, and *Aag2.TET* cells were gifts from the McGraw laboratory, Monash University, Australia. Tetracycline treatment was used to abolish *wMel* from the *Aag2.wMel* cells to prepare *Aag2.TET* cells (44). All *A. aegypti* mosquitoes (*wMel* and TET lines) were reared and maintained as described previously (6).

Zika virus strain stocks were gifts from Julian Druce, Victorian Infectious Diseases Reference Laboratory, Melbourne, Australia. Zika African strain (GenBank accession no. KU963573.2) was isolated from Uganda while the Asian strain was isolated from a local patient who had just returned from the Pacific. The DENV-1 (GenBank accession no. FJ432734) and the DENV-2 Cosmopolitan strains were gifts from Oxford University Clinical Research Unit, Vietnam. All viruses were expanded by inoculation into C6/36 cells with a multiplicity of infection (MOI) of 0.1 and collection of culture supernatant 7 d postinfection following filtration. All viral isolates included in this study were passaged less than six times. Infectious titers were determined by plaque assay. Infectivity was measured using plaque assay and qRT-PCR analysis of viral genomes.

**Liquid Chromatography–Mass Spectrometry.** For LCMS analysis, metabolites in both polar and nonpolar phase extracts were analyzed by LCMS in positive ionization mode to obtain the most comprehensive coverage. The levels were then compared to internal standard controls and ratios between infected and uninfected cells determined.

To ensure that the lipidomic profile of the cells accurately represented the infected environment, supernatant from the infected cells was evaluated by plaque assay for virus titers to confirm infection, before proceeding with

LCMS. Cells were washed with  $1\times$  PBS and quenched by adding liquid nitrogen to completely cover the cells (45). Upon evaporation of the liquid nitrogen,  $600\ \mu\text{L}$  of 1:9 chloroform:methanol (vol/vol) containing  $10\ \mu\text{g/mL}$  of each internal standard (PC19:0/19:0 [part 850367], PE-d31 [part 860374], PG17:0/17:0 [part 830456], DG-d5 1,3-15:0/15:0 [part 110536] and TG-d5 19:0/12:0/19:0 [part 8609040], Avanti Polar Lipids) was added and incubated for 10 min at room temperature (45). Cells were scraped, and the extract along with the cell debris was transferred to microfuge tubes and stored at  $-80\ ^\circ\text{C}$  until further processing (45). Samples were centrifuged at  $16,100\times g$  (Beckman Coulter Microfuge 22R Refrigerated Microcentrifuge) for 10 min and the supernatant transferred to fresh tube (45). The pellet was further extracted with  $200\ \mu\text{L}$  of 1:1 chilled chloroform:methanol (vol/vol) with vortexing for 30 min at room temperature and sonication for 10 min followed by centrifugation and the supernatant combined with the first extract (45). The combined supernatants were transferred into glass inserts and dried in a vacuum concentrator (Christ RVC 2-33) (45). Sample were reconstituted with  $200\ \mu\text{L}$  of methanol:water-saturated butanol (1.2:8.8, vol/vol) mixture (45). Pooled biological quality control samples were prepared by pooling aliquots of the extracts from each sample and ran after every five samples (45).

Lipids were analyzed according to ref. 45 using an Agilent 1290 LC system and Agilent Triple Quadrupole 6490 mass spectrometer (MS). Briefly, lipids were separated by injecting  $1\ \mu\text{L}$  of the sample onto a  $100\ \text{mm}\times 2.1\ \text{mm}\times 1.8\ \mu\text{m}$  Zorbax Eclipse Plus C-18 column (Agilent Technologies) followed by elution at flow rate of  $0.4\ \text{mL/min}$  using a solvent system of A: water/acetonitrile/isopropanol (50:30:20, vol/vol/vol) and B: water/acetonitrile/isopropanol (1.9:90, vol/vol/vol), with a total run time of 14 min. Lipids were quantified by electrospray ionization-mass spectrometry using multiple reaction monitoring with capillary voltage  $3,500\ \text{V}$ , fragmentor voltage  $380\ \text{V}$ , collision energy  $15\text{--}60\ \text{V}$ , and collision gas (nitrogen) at  $17\ \text{L/min}$ . Quantitation was based on relative changes in peak areas. Data processing was performed using Agilent's Mass Hunter Quantitative Analysis (QQQ) software.

**Plaque Assay.** Serial dilutions (10-fold) of virus were added to BHK-21 cells in 24-well plates and incubated for 1 h at  $37\ ^\circ\text{C}$ . Media was aspirated and replaced with 0.8% methyl-cellulose in maintenance medium (RPMI-1640, 2% fetal calf serum (FCS), 25 mM HEPES, penicillin, and streptomycin). After 6 d at  $37\ ^\circ\text{C}$ , cells were fixed with 20% formaldehyde at room temperature for 20 min and washed with water, and 1 mL of 1% crystal violet was added for 20 min. The plates were washed and dried, and the plaque-forming units per milliliter were calculated.

**Quantification of RNA.** Total RNA from virus-infected cells was extracted using the RNeasy kit (Qiagen). Superscript III reverse transcriptase and random hexamers (Invitrogen) were used in the reverse transcription reactions to generate cDNA. qRT-PCR was performed using the iQ SYBR Green Supermix Kit (Bio-Rad) and LightCycler 480 SYBR Green I Master mix, according to the manufacturer's instructions. Quantification of DENV levels was performed as previously described (46). Primers used for Zika virus detection are as follows: Zika4481 F (CTGTGGCATGAACCAATAG) and Zika4552c R (ATCCCAKAGRGACCACCTCC). They bind universally to both strains of Zika virus used in this study. All PCRs were normalized against GAPDH. Reactions were run on a Roche Lightcycler 480 (Roche), and data analysis was carried out with the Lightcycler 480 software. qRT-PCR conditions to detect viral RNA:  $95\ ^\circ\text{C}$  for 5 min, followed by 45 cycles of  $95\ ^\circ\text{C}$  for 10 s,  $55\ ^\circ\text{C}$  for 5 s, and  $72\ ^\circ\text{C}$  for 10 s. Cycling conditions for the quantification of immune genes:  $95\ ^\circ\text{C}$  for 5 min, followed by 45 cycles of  $95\ ^\circ\text{C}$  for 5 s,  $53\ ^\circ\text{C}$  for 10 s, and  $72\ ^\circ\text{C}$  for 10 s.

**Calculation of *Wolbachia* Density.** *Wolbachia* density in cells was determined by comparing the abundance of *Wolbachia TM513* gene to that of the single-copy mosquito *rps17* gene using relative qPCR. *Aag2.wMel* and *Aag2.TET* cells were first lysed with squash extraction buffer (10 mM Tris Buffer, 1 mM ethylenediamine tetraacetic acid [EDTA], 50 mM NaCl in milli-Q water, 30  $\mu\text{L}$  of Proteinase K). Cell lysates were then incubated at  $56\ ^\circ\text{C}$  for 5 min, followed by  $98\ ^\circ\text{C}$  for 5 min and spun down at full speed for 1 min to remove the supernatant. The qPCR was performed with  $1\ \mu\text{L}$  of the supernatant using the LightCycler 480 SYBR Green I Master mix, according to the manufacturer's instructions. Probes and primers used are as described: For *wMel* detection, TM513 F (5'-CAAATTGCTCTTGTCTGTGG-3'), TM 513 R (5'-GGGTGTTAAGCAGAGTTACGG-3'), and TM513 Cy5 probe (5'-TGAAATGGAAAAATGGCGAGGTAGG-3') were used. To detect the housekeeping gene, RPS 17 F (5'-TCCGTGGTATCTCCATCAAGCT-3'), RPS 17 R (5'-CACTTC-CGGACGTAGTTGC-3'), and RPS 17 FAM probe (5'-CAGGAGGAGGAAACGT-GAGCGCAG-3') were utilized. PCR cycling conditions were  $95\ ^\circ\text{C}$  for 5 min, 45 cycles of  $95\ ^\circ\text{C}$  for 10 s,  $60\ ^\circ\text{C}$  for 15 s,  $72\ ^\circ\text{C}$  for 1 s, followed by cooling at  $40\ ^\circ\text{C}$  for 10 s.

*Wolbachia* density was quantified for the *A. aegypti* mosquitoes used in the Etomoxir-treatment experiment. At 3 d postemergence, 16 individual females from each sample group were dissected to separate the heads from the abdomens/thoraxes. DNA was then extracted using the QIAcube HT purification kit (Qiagen), according to manufacturer's instructions. *Wolbachia* density was then determined by qRT-PCR by comparing the abundance of *wsp* (*Wolbachia surface protein*) gene to that of the single-copy mosquito *rps17* gene. *Rps17* primers were as above. *Wsp* primers were *wsp* F (5'-CTG GTGTTAGTTATGATGAAC-3' and *wsp* R (5'-AAAAATTAACGCTACTCCA-3'). For each sample, qPCR amplification of DNA was performed in duplicate with a LightCycler 480 II Instrument (Roche) using LightCycler Multiplex RNA Virus Master (Roche) according to the manufacturer's protocol. The temperature profile of the qPCR was 10 min of preincubation at 95 °C, 45 cycles of 95 °C for 10 s, 60 °C for 15 s, 72 °C for 10 s. *wsp:rps17* ratios were obtained for each biological replicate using the LightCycler 480 II software (Roche) and then compared independently for each sample.

**Mosquito Microinjections.** Adult microinjections were performed as previously described using DENV-2 Cosmopolitan strain,  $3.4 \times 10^5$  TCID<sub>50</sub>/mL (6). Quantification of DENV-2 genomic copies was done on whole mosquitoes using the DENV 3'UTR primer/probe set, as previously described (6).

**Fluorescent In Situ Hybridization.** Aag-2 cells were seeded in an eight-well chamber slide (Lab-Tek) and incubated overnight at 25 °C. Fluorescent in situ hybridization was carried out using *wMel*-specific 16S 22 rRNA probes as described previously (4). The Zeiss LSM710 confocal microscope was used for imaging.

#### Pharmacological Agent Studies.

**Etomoxir (Sigma).** A widely used inhibitor, etomoxir is an irreversible inhibitor of the enzyme carnitine palmitoyltransferase-1 (CPT-1) that converts fatty acyl-CoAs in the cytoplasm into acyl-carnitines (32, 33). This prevents the formation of acyl-carnitines, thus strongly inhibiting mitochondrial  $\beta$ -oxidation. Cytotoxicity was assessed by serial dilution of etomoxir on HuH-7 cells and viability assessed with the CytoTox 96 Non-Radioactive Cytotoxicity Assay (Promega). Nile red staining was performed as described to confirm that the drug is effective (47, 48). For the experiment, HuH-7 cells were treated with media containing 200  $\mu$ M etomoxir for 48 h, after which virus was added at MOI 5. Inoculum was removed after 2 h, and fresh media was added. Both supernatant and infected cells were removed after 24 h for plaque assay and qRT-PCR, respectively. Treatment experiments were performed in mosquitoes

by rearing the larvae in 100  $\mu$ M etomoxir-treated water. *Wolbachia* density was measured at 3 d postemergence of mosquitoes.

**Acyl-carnitines 12:0, 16:0, and 18:1 (Avanti Polar Lipids).** Rescue experiments were conducted by mixing all three commercially available carnitines, C12:0 carnitine (part 870850), C16:0 carnitine (part 870851), and C18:1 carnitine (part 870852) each at a concentration of 25  $\mu$ M as described, and adding them to infected cells 24 h.p.i (49). Samples were harvested at 96 h.p.i. and virus titers/RNA levels determined.

**Western blot analysis.** Mouse anti-*Wolbachia* WSP antibody was obtained from Bei Resources. Mouse anti-dengue-E (clone 4G2) and mouse anti-flavivirus NS1 (clone 4G4) were generously provided by Ooi Eng Eong (Duke-National University of Singapore Medical School, Singapore) and Roy Hall (University of Queensland, Brisbane, Australia) respectively. Briefly, infected cells were lysed with Nonidet P-40 lysis buffer containing protease inhibitors and loaded on a Bis/Tris polyacrylamide gel. Proteins were transferred to a Hi-Bond enhanced chemiluminescence nitrocellulose membrane and incubated with primary antibodies overnight at 4 °C. Membranes were incubated with species-specific secondary antibodies conjugated to either Alexa Fluor 488 or 647, and proteins were detected with the Bio-Rad Pharos FX system.

**Cellular ATP assay.** Measurement of cellular ATP levels were performed using the Luminescent ATP Detection Assay kit (Abcam) as per manufacturer's instructions.

**Statistical Analysis.** For LCMS, each metabolite was first normalized to the median of the sample. The interaction between bacteria and virus (i.e., all four datasets: bacteria<sup>+/−</sup> and virus<sup>+/−</sup>) were analyzed using a two-way ANOVA test. Results of the ANOVA tests were controlled for false positives using the Benjamini-Hochberg method (50). All results are presented as mean  $\pm$  SD of at least three independent experiments, unless otherwise indicated. Data were analyzed using unpaired, two-tailed Student's *t* test or two-way ANOVA and considered significant if  $P < 0.05$  ( $*P < 0.05$ ;  $**P < 0.01$ ;  $***P < 0.001$ ;  $****P < 0.0001$ ).

**Data Availability.** The authors declare that the data supporting the findings of this study are available within the [SI Appendix](#) files.

**ACKNOWLEDGMENTS.** This work was supported by the Wellcome Trust (UK) and the National Health and Medical Research Council (Australia). We thank Dr. Elizabeth A. McGraw for providing the *A. aegypti* cells and protocols used in maintaining the *wMel* cell lines. They also thank Drs. Brunda Nijagal and Kirsty McPherson for their invaluable advice throughout this work.

- H. L. Dutra *et al.*, *Wolbachia* blocks currently circulating Zika virus isolates in Brazilian *Aedes aegypti* mosquitoes. *Cell Host Microbe* **19**, 771–774 (2016).
- S. L. O'Neill *et al.*, Scaled deployment of *Wolbachia* to protect the community from dengue and other *Aedes* transmitted arboviruses. *Gates Open Res.* **2**, 36 (2019).
- M. T. Aliota, S. A. Peinado, I. D. Velez, J. E. Osorio, The *wMel* strain of *Wolbachia* reduces transmission of Zika virus by *Aedes aegypti*. *Sci. Rep.* **6**, 28792 (2016).
- L. A. Moreira *et al.*, A *Wolbachia* symbiont in *Aedes aegypti* limits infection with dengue, Chikungunya, and Plasmodium. *Cell* **139**, 1268–1278 (2009).
- T. H. Ant, C. S. Herd, V. Geoghegan, A. A. Hoffmann, S. P. Sinkins, The *Wolbachia* strain *wAu* provides highly efficient virus transmission blocking in *Aedes aegypti*. *PLoS Pathog.* **14**, e1006815 (2018).
- J. E. Fraser *et al.*, Novel *Wolbachia*-transinfected *Aedes aegypti* mosquitoes possess diverse fitness and vector competence phenotypes. *PLoS Pathog.* **13**, e1006751 (2017).
- A. A. Hoffmann, P. A. Ross, G. Rašić, *Wolbachia* strains for disease control: Ecological and evolutionary considerations. *Evol. Appl.* **8**, 751–768 (2015).
- D. A. Joubert *et al.*, Establishment of a *Wolbachia* superinfection in *Aedes aegypti* mosquitoes as a potential approach for future resistance management. *PLoS Pathog.* **12**, e1005434 (2016).
- K. L. Anders *et al.*, The AWED trial (Applying *Wolbachia* to Eliminate Dengue) to assess the efficacy of *Wolbachia*-infected mosquito deployments to reduce dengue incidence in Yogyakarta, Indonesia: Study protocol for a cluster randomised controlled trial. *Trials* **19**, 302 (2018).
- L. B. Carrington *et al.*, Field- and clinically derived estimates of *Wolbachia*-mediated blocking of dengue virus transmission potential in *Aedes aegypti* mosquitoes. *Proc. Natl. Acad. Sci. U.S.A.* **115**, 361–366 (2018).
- E. C. Pacidônio, E. P. Caragata, D. M. Alves, J. T. Marques, L. A. Moreira, The impact of *Wolbachia* infection on the rate of vertical transmission of dengue virus in Brazilian *Aedes aegypti*. *Parasit. Vectors* **10**, 296 (2017).
- K. Servick, Winged warriors. *Science* **354**, 164–167 (2016).
- M. Hussain, F. D. Frentiu, L. A. Moreira, S. L. O'Neill, S. Asgari, *Wolbachia* uses host microRNAs to manipulate host gene expression and facilitate colonization of the dengue vector *Aedes aegypti*. *Proc. Natl. Acad. Sci. U.S.A.* **108**, 9250–9255 (2011).
- J. Martinez *et al.*, Symbionts commonly provide broad spectrum resistance to viruses in insects: A comparative analysis of *Wolbachia* strains. *PLoS Pathog.* **10**, e1004369 (2014).
- X. Pan *et al.*, *Wolbachia* induces reactive oxygen species (ROS)-dependent activation of the Toll pathway to control dengue virus in the mosquito *Aedes aegypti*. *Proc. Natl. Acad. Sci. U.S.A.* **109**, E23–E31 (2012).
- E. Rancès, Y. H. Ye, M. Woolfit, E. A. McGraw, S. L. O'Neill, The relative importance of innate immune priming in *Wolbachia*-mediated dengue interference. *PLoS Pathog.* **8**, e1002548 (2012).
- G. Zhang, M. Hussain, S. L. O'Neill, S. Asgari, *Wolbachia* uses a host microRNA to regulate transcripts of a methyltransferase, contributing to dengue virus inhibition in *Aedes aegypti*. *Proc. Natl. Acad. Sci. U.S.A.* **110**, 10276–10281 (2013).
- P. Lu, G. Bian, X. Pan, Z. Xi, *Wolbachia* induces density-dependent inhibition to dengue virus in mosquito cells. *PLoS Negl. Trop. Dis.* **6**, e1754 (2012).
- E. P. Caragata *et al.*, Dietary cholesterol modulates pathogen blocking by *Wolbachia*. *PLoS Pathog.* **9**, e1003459 (2013).
- V. Geoghegan *et al.*, Perturbed cholesterol and vesicular trafficking associated with dengue blocking in *Wolbachia*-infected *Aedes aegypti* cells. *Nat. Commun.* **8**, 526 (2017).
- J. C. Molloy, U. Sommer, M. R. Viant, S. P. Sinkins, *Wolbachia* modulates lipid metabolism in *Aedes albopictus* mosquito cells. *Appl. Environ. Microbiol.* **82**, 3109–3120 (2016).
- Y. H. Ye, M. Woolfit, E. Rancès, S. L. O'Neill, E. A. McGraw, *Wolbachia*-associated bacterial protection in the mosquito *Aedes aegypti*. *PLoS Negl. Trop. Dis.* **7**, e2362 (2013).
- S. Liebscher *et al.*, Phospholipase A2 activity during the replication cycle of the flavivirus West Nile virus. *PLoS Pathog.* **14**, e1007029 (2018).
- N. Nasheri *et al.*, Modulation of fatty acid synthase enzyme activity and expression during hepatitis C virus replication. *Chem. Biol.* **20**, 570–582 (2013).
- R. Perera *et al.*, Dengue virus infection perturbs lipid homeostasis in infected mosquito cells. *PLoS Pathog.* **8**, e1002584 (2012).
- T. E. Aktepe, S. Liebscher, J. E. Prier, C. P. Simmons, J. M. Mackenzie, The host protein reticulon 3.1A is utilized by flaviviruses to facilitate membrane remodelling. *Cell Rep.* **21**, 1639–1654 (2017).
- N. S. Heaton *et al.*, Dengue virus nonstructural protein 3 redistributes fatty acid synthase to sites of viral replication and increases cellular fatty acid synthesis. *Proc. Natl. Acad. Sci. U.S.A.* **107**, 17345–17350 (2010).
- J. M. Mackenzie, A. A. Khromykh, R. G. Parton, Cholesterol manipulation by West Nile virus perturbs the cellular immune response. *Cell Host Microbe* **2**, 229–239 (2007).

29. C. Rothwell *et al.*, Cholesterol biosynthesis modulation regulates dengue viral replication. *Virology* **389**, 8–19 (2009).
30. N. Chotiwan *et al.*, Dynamic remodeling of lipids coincides with dengue virus replication in the midgut of *Aedes aegypti* mosquitoes. *PLoS Pathog.* **14**, e1006853 (2018).
31. M. A. Martín-Acebes *et al.*, The composition of West Nile virus lipid envelope unveils a role of sphingolipid metabolism in flavivirus biogenesis. *J. Virol.* **88**, 12041–12054 (2014).
32. L. S. Pike, A. L. Smift, N. J. Croteau, D. A. Ferrick, M. Wu, Inhibition of fatty acid oxidation by etomoxir impairs NADPH production and increases reactive oxygen species resulting in ATP depletion and cell death in human glioblastoma cells. *Biochim. Biophys. Acta* **1807**, 726–734 (2011).
33. B. W. Wong *et al.*, The role of fatty acid  $\beta$ -oxidation in lymphangiogenesis. *Nature* **542**, 49–54 (2017).
34. L. M. Genty, D. Bouchon, M. Raimond, J. Bertaux, *Wolbachia* infect ovaries in the course of their maturation: Last minute passengers and priority travellers? *PLoS One* **9**, e94577 (2014).
35. N. S. Heaton, G. Randall, Dengue virus-induced autophagy regulates lipid metabolism. *Cell Host Microbe* **8**, 422–432 (2010).
36. L. O. Fernandes-Siqueira, J. D. Zeidler, B. G. Sousa, T. Ferreira, A. T. Da Poian, Anaplerotic role of glucose in the oxidation of endogenous fatty acids during Dengue virus infection. *MSphere* **3**, e00458-17 (2018).
37. N. Tongluan *et al.*, Involvement of fatty acid synthase in dengue virus infection. *Virology* **14**, 28 (2017).
38. R. I. Klein Geltink *et al.*, Mitochondrial priming by CD28. *Cell* **171**, 385–397.e11 (2017).
39. V. Zuzarte-Luis *et al.*, Dietary alterations modulate susceptibility to Plasmodium infection. *Nat. Microbiol.* **2**, 1600–1607 (2017).
40. N. Fattouh, C. Cazevielle, F. Landmann, *Wolbachia* endosymbionts subvert the endoplasmic reticulum to acquire host membranes without triggering ER stress. *PLoS Negl. Trop. Dis.* **13**, e0007218 (2019).
41. G. Haqshenas *et al.*, A role for the insulin receptor in the suppression of Dengue virus and Zika virus in *Wolbachia*-infected mosquito cells. *Cell Rep.* **26**, 529–535.e3 (2019).
42. M. G. Schooneman, F. M. Vaz, S. M. Houten, M. R. Soeters, Acylcarnitines: Reflecting or inflicting insulin resistance? *Diabetes* **62**, 1–8 (2013).
43. S. A. Ritchie, *Wolbachia* and the near cessation of dengue outbreaks in Northern Australia despite continued dengue importations via travellers. *J. Travel Med.* **25**, tay084 (2018).
44. F. D. Frentiu, J. Robinson, P. R. Young, E. A. McGraw, S. L. O'Neill, *Wolbachia*-mediated resistance to dengue virus infection and death at the cellular level. *PLoS One* **5**, e13398 (2010).
45. K. Huynh *et al.*, Lipidomic profiling of murine macrophages treated with fatty acids of varying chain length and saturation status. *Metabolites* **8**, E29 (2018).
46. G. Manokaran *et al.*, Dengue subgenomic RNA binds TRIM25 to inhibit interferon expression for epidemiological fitness. *Science* **350**, 217–221 (2015).
47. A. Herms *et al.*, Cell-to-cell heterogeneity in lipid droplets suggests a mechanism to reduce lipotoxicity. *Curr. Biol.* **23**, 1489–1496 (2013).
48. A. Herms *et al.*, AMPK activation promotes lipid droplet dispersion on deetyrosinated microtubules to increase mitochondrial fatty acid oxidation. *Nat. Commun.* **6**, 7176 (2015).
49. H. Deguchi *et al.*, Acylcarnitines are anticoagulants that inhibit factor Xa and are reduced in venous thrombosis, based on metabolomics data. *Blood* **126**, 1595–1600 (2015).
50. Y. Benjamini, Y. Hochberg, Controlling the false discovery rate: A practical and powerful approach to multiple testing. *J. R. Stat. Soc. Ser. A Stat. Soc.* **57**, 289–300 (1995).